Latent HIV reservoirs exhibit inherent resistance to elimination by CD8+ T cells

Szu-Han Huang,[1] Yanqin Ren,[1] Allison S. Thomas,[1] Dora Chan,[1] Stefanie Mueller,[2] Adam R. Ward,[1] Shabnum Patel,[1,3] Catherine M. Bollard,[1,3] Conrad Russell Cruz,[1,3] Sara Karandish,[1] Ronald Truong,[1] Amanda B. Macedo,[1] Alberto Bosque,[1] Colin Kovacs,[4] Erika Benko,[4] Alicja Piechocka-Trocha,[2] Hing Wong,[5] Emily Jeng,[5] Douglas F. Nixon,[1] Ya-Chi Ho,[6] Robert F. Siliciano,[6,7] Bruce D. Walker,[2,7,8] and R. Brad Jones[1,2]

[1]Department of Microbiology, Immunology and Tropical Medicine, The George Washington University, Washington DC, USA. [2]Ragon Institute of Massachusetts Institute of Technology (MIT), Massachusetts General Hospital (MGH), and Harvard University, Cambridge, Massachusetts, USA. [3]Children's National Health System, Washington DC, USA. [4]Maple Leaf Medical Clinic, Toronto, Ontario, Canada. [5]Altor Bioscience Corporation, Miramar, Florida, USA. [6]Department of Medicine, Johns Hopkins University School of Medicine, Baltimore, Maryland, USA. [7]Howard Hughes Medical Institute, Chevy Chase, Maryland, USA. [8]Institute for Medical Engineering and Sciences, MIT, Cambridge, Massachusetts, USA.

The presence of persistent, latent HIV reservoirs in CD4+ T cells obstructs current efforts to cure infection. The so-called kick-and-kill paradigm proposes to purge these reservoirs by combining latency-reversing agents with immune effectors such as cytotoxic T lymphocytes. Support for this approach is largely based on success in latency models, which do not fully reflect the makeup of latent reservoirs in individuals on long-term antiretroviral therapy (ART). Recent studies have shown that CD8+ T cells have the potential to recognize defective proviruses, which comprise the vast majority of all infected cells, and that the proviral landscape can be shaped over time due to in vivo clonal expansion of infected CD4+ T cells. Here, we have shown that treating CD4+ T cells from ART-treated individuals with combinations of potent latency-reversing agents and autologous CD8+ T cells consistently reduced cell-associated HIV DNA, but failed to deplete replication-competent virus. These CD8+ T cells recognized and potently eliminated CD4+ T cells that were newly infected with autologous reservoir virus, ruling out a role for both immune escape and CD8+ T cell dysfunction. Thus, our results suggest that cells harboring replication-competent HIV possess an inherent resistance to CD8+ T cells that may need to be addressed to cure infection.

Introduction

Eradicating latent HIV reservoirs will require the elimination of persistent populations of cells with integrated HIV proviruses. The major barrier impeding viral eradication is thought to be a reservoir of latently infected resting CD4+ T cells (1–3). While in a quiescent state, these cells are not thought to express HIV antigens, and thus cannot be targeted by the immune system. The so-called kick-and-kill paradigm proposes to combine latency-reversing agents (LRAs) with immune effectors, such as CD8+ T cells, to both overcome this quiescent state and eliminate infected cells (4, 5).

The extremely low frequencies of HIV-infected cells present in peripheral blood mononuclear cells (PBMCs) from antiretroviral therapy–treated (ART-treated) individuals (~1 inducible infectious unit per 10^6 CD4+ T cells) presents a significant challenge to testing eradication strategies. This has motivated the use of latency models, such as primary resting CD4+ T cells that have been infected with HIV in vitro (6–8). The kick-and-kill paradigm gained traction when it was demonstrated that latency reversal (kick) alone, with the LRA vorinostat, was insufficient to cause the death of infected cells in a postactivation in vitro latency model, whereas the addition of expanded HIV-specific CD8+ T cells resulted in infected cell elimination (5). Others have since reported similar results using additional in vitro latency models, combined with natural or engineered CD8+ T cells, or NK cells as effectors (9–14). These results have motivated the translation of the kick-and-kill approach into clinical trials that, thus far, have failed to achieve reductions in infectious viral reservoirs (15–17). This lack of efficacy has generally been attributed to insufficient latency reversal and/or to suboptimal immune clearance, with substantial clinical efforts currently focused on enhancing these factors. The current study raises the alternative possibility that natural HIV reservoirs in ex vivo CD4+ T cells may possess additional barriers to CD8+ T cell–mediated elimination that are not reflected in latency models.

Although in vitro latency models have led to valuable insights, they do not fully reflect the complex makeup of the latently infected cells that arise over years and decades in ART-treated individuals. Over these time frames, the compositions of infected cell populations are shaped by clonal expansion of cells harboring both defective and intact proviruses (18–22). Since overall frequencies of infected cells remain fairly constant (23, 24), this expansion must be counterbalanced by the death of other cells. Emerging evidence suggests that this process may select for resilient clones of infected cells. In primary-cell models of latency, where no selection has occurred, strong LRAs including PMA/ionomycin (PMA/I) and T cell receptor agonists are sufficient to

Conflict of interest: H. Wong and E. Jeng are employees of Altor Bioscience Corporation, which manufactures ALT-803, the IL-15 superagonist used in this study.
Submitted: September 18, 2017; **Accepted:** December 5, 2017.
Reference information: *J Clin Invest.* https://doi.org/10.1172/JCI97555.

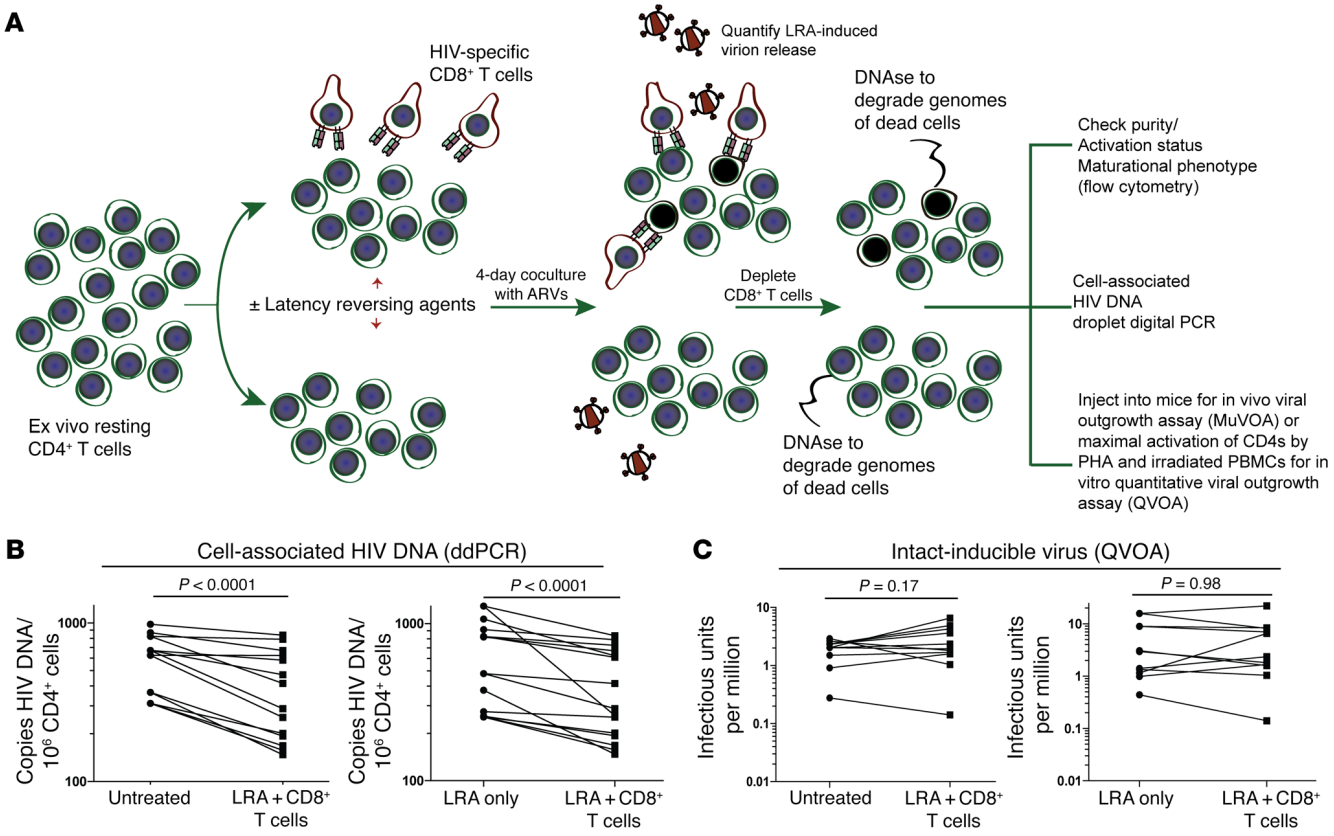

Figure 1. HIV eradication (HIVE) assays. (**A**) Schematic of the HIVE assay. (**B**) Comparison of the 10 HIVE assays in this study, between either untreated or LRA-only levels of HIV DNA, with levels after treatment with LRA + CD8+ T cells. (**C**) Comparison of the same 10 HIVE assays in this study between both untreated and LRA-only IUPMs, with those after treatment with LRA + CD8+ T cells.

drive the elimination of infected cells by cytopathic effects (25, 26). In contrast, stimulation of ex vivo CD4+ T cells with PMA/I results in sustained viral production and further proliferation of infected-cell clones (27). This resiliency of ex vivo reservoirs has been linked to insertional mutagenesis as a result of proviral integration. Over years of ART, there is in vivo selection for infected-cell clones with integrations into genes associated with enhanced proliferation and/or survival (18, 19). Given such complexities, we perceived a need to extend testing of CD8+ T cell–based kick-and-kill strategies from latency models to ex vivo patient CD4+ T cells.

In the current study, we utilized a newly designed assay to test whether the coculture of potent CD8+ T cell effectors in combination with LRAs could drive reductions in latent HIV reservoirs from the ex vivo CD4+ T cells of ART-treated individuals. Our study applies a standard quantitative viral outgrowth assay (QVOA) (with mitogenic reactivation of latent virus) to assess viral reservoir reductions following ex vivo kick-and-kill approaches. QVOAs rely on limiting dilutions of replicates of stimulated CD4+ T cells to calculate maximal likelihood estimates of infectious units per million cells (IUPM) (2, 23, 28). Furthermore, QVOAs strictly measure replication-competent virus, while HIV DNA, p24 antigen, or viral RNA assays may be confounded by the presence of defective proviruses (29, 30). Upon treating ex vivo CD4+ T cells with combinations of CD8+ T cells and LRAs, we observed consistent reductions in levels of HIV DNA that, surprisingly, were not accompanied by reductions in infectious viral reservoirs as measured by QVOA. This failure to reduce infectious reservoirs was observed even in the context of potent LRAs, and was not attributable to immune escape. Our results suggest the elimination of a subset of cells harboring defective HIV proviruses, while those harboring infectious proviruses displayed a resistance to CD8+ T cell–mediated killing that has not been observed in latency models, and which may have to be overcome to cure infection.

Results

Validation of HIV eradication assay using primary cell model of latency. We developed an ex vivo HIV eradication (HIVE) assay to test the abilities of CD8+ T cells to kill reactivated natural HIV reservoirs. The schematic of this assay is given in Figure 1A. Briefly, CD4+ T cells from ART-treated individuals were isolated from leukapheresis samples, treated with LRAs, and then cocultured for 4 days with autologous immune effectors in the presence of antiretrovirals and DNAse (to degrade the genomes of dead cells). CD4+ T cells were then repurified from these cocultures and subjected to phenotypic characterization (Supplemental Figure 1 and Supplemental Table 1), quantification of residual cell-associated HIV DNA by digital droplet PCR (ddPCR), and QVOAs to measure the frequencies of cells harboring intact-inducible proviruses (i.e., those that give rise to viral replication following a single round of maximal stimulation; see ref. 31). The output of this assay is a maximal likelihood estimate of IUPM with a 95% confidence interval (Supplemental Figure 2) (28).

Before applying this assay to ex vivo CD4+ T cells, we performed validation experiments on a primary cell model of post-activation latency (32, 33) to determine whether it could reliably measure changes in levels of both HIV DNA and IUPM. Infected cells of this latency model were spiked into autologous ex vivo CD4+ T cells to generate target cell populations, approximating the infected cell frequencies found in patient samples. A recent study has demonstrated that the BCL-2 inhibitor ABT-199 substantially enhanced the death of HIV-infected cells following latency reversal, by potentiating viral cytopathicity (34). We therefore tested whether the combination of the LRA bryostatin and ABT-199 would eliminate latently infected cells in this model system. We observed that treatment with bryostatin alone led to significant decreases in both levels of HIV DNA and IUPM (Supplemental Figure 3, $P < 0.0001$ and $P = 0.003$, respectively). This is consistent with previous studies, which have indicated that potent LRAs alone are sufficient to drive some elimination of infected cells in this and other models of latency (5, 32). As expected, substantially greater reductions in levels of both HIV DNA and IUPM were observed following combination treatment with bryostatin and ABT-199 (Supplemental Figure 3, $P = 0.0009$ and $P < 0.0001$, respectively, compared with bryostatin alone). Thus, decreases in levels of both HIV DNA and IUPM can be effectively measured in HIVE assays.

Compiled results — combinations of HIV-specific CD8+ T cells and LRAs reduce HIV DNA, but not infectious reservoirs from ex vivo CD4+ T cells. The remainder of this study focused on testing the abilities of combinations of LRAs and autologous CD8+ T cell effectors to eliminate HIV-infected cells from the ex vivo CD4+ T cells of ART-treated individuals. We have taken the approach of first presenting compiled data from all experiments together in order to illustrate overall trends (Figure 1, B and C), and then delving into details of individual experiments (Figures 2–5, and Supplemental Figures 2 and 4). Demographic and clinical information for study participants are given in Table 1. Overall, we observed that combinations of LRAs with either HIV-specific CD8+ T cell lines or clones consistently drove significant reductions in proviral HIV DNA in autologous CD4+ T cells, as compared with no treatment or LRA-only conditions ($P < 0.0001$, Figure 1B). Surprisingly, this was not accompanied by a significant reduction in intact-inducible virus (as measured by QVOA) in any single experiment. In fact, we observed an overall trend towards increases in IUPM when comparing LRA plus CD8+ T cell or CD8+ T cell line conditions with untreated controls ($P = 0.17$, Figure 1C). These results stand in contrast to those of the primary cell model of latency in which we observed that levels of HIV DNA and IUPM decreased in parallel, and where even the use of a strong LRA alone was sufficient to drive significant reductions in both measures (Supplemental Figure 3). The results given below represent detailed profiles of the individual experiments encompassed by the above summary, allowing detailed examination of this unexpected result.

Ex vivo CD8+ T cells and short-term-expanded HIV-specific CD8+ T cell lines reduce HIV DNA without measurably impacting infectious reservoirs. We first applied the HIVE assay to assess the ability of ex vivo CD8+ T cells to eliminate autologous, latently infected ex vivo CD4+ T cells, when combined with the following LRAs: an IL-15 superagonist (IL-15SA, comprising a mutated form of IL-15 with enhanced activity bound to an IL-15Rα–Fc fusion protein; see ref. 35); and Pam_3CSK_4, a Toll-like receptor 2 (TLR2) agonist (8). We selected these LRAs based on our previous observations that they both induce T cell recognition of latently infected cells, and directly enhance multiple T cell functions, including cytotoxicity (36). Experiments were performed on cells from 2 ART-treated individuals with strong ex vivo HIV-specific CD8+ T cell responses as determined by ELISPOT (OM5334, 1,758 SFU/10^6 PBMCs; OM5011, 1,345 SFU/10^6 PBMCs; see Supplemental Text for further clinical histories and T cell response characterization). For both individuals, we observed significant reductions in levels of HIV DNA in ex vivo CD4+ T cells following treatment with LRAs and ex vivo autologous CD8+ T cells (Figure 2, A and C).

In the initial experiment with OM5334, we expected that this clear reduction in levels of HIV DNA would be accompanied by a marked reduction in the infectious latent HIV reservoir. We therefore utilized a previously described in vivo murine viral outgrowth assay (MuVOA) (37) to assess any remaining infectious virus, given that the MuVOA may be more sensitive than a QVOA (38). For each treatment group, 3 naive NOD-SCID IL-2Rγ$^{-/-}$ (NSG) mice were injected with 10^7 repurified CD4+ T cells from HIVE assays (corresponding to those measured in Figure 2A) and viral loads were measured weekly. Unexpectedly, we observed viral rebound in all animals within 1 week, indicating that infectious virus had not been sufficiently reduced ex vivo to delay viral rebound (Figure 2B). Note that we would caution against drawing conclusions from relative viral load levels following rebound in this model, as these are unstable and influenced by fluctuations in the nascent CD4 grafts (i.e., robust viral replication can deplete these early CD4 grafts, leading to drops in viral load; see ref. 37). Given this result of contemporaneous viral rebound between groups, we moved to assessing infectious viral reservoirs by in vitro viral outgrowth assays in all subsequent experiments in order to detect more subtle changes in infectious reservoirs. For the HIVE assay using autologous CD8+ T cells from participant OM5011, the significant reduction in levels of HIV DNA observed in Figure 2C was not associated with a measurable reduction in IUPM (Figure 2D).

We next tested whether enhancing HIV-specific CD8+ T cell responses through a short-term expansion in response to HIV peptides and cytokines would facilitate reductions in the autologous infectious reservoir, using cells from a third study participant, CIRC0311. The resulting HIV-specific T cell line exhibited potent responses by IFN-γ ELISPOT, distributed across at least 7 epitopes in Nef, Gag, and Pol (Supplemental Figure 4). As with ex vivo CD8+ T cells, we observed that the combination of this expanded HIV-specific T cell line with an IL-15SA drove significant reductions in HIV DNA ($P < 0.001$, Figure 2E), with a similar reduction observed when combined with the LRA bryostatin ($P = 0.02$, Figure 2E). However, neither of these combinations drove a reduction in the intact-inducible reservoir, as measured by QVOA (Figure 2F).

The failure of ex vivo HIV-specific T cells to reduce infectious virus in the above experiments may have resulted from a number of factors, including immune escape at targeted epitopes in intact proviruses, poor effector function of CD8+ T cells, or insufficient latency reversal. We therefore moved to the use of CD8+ T cell clones to define the potential roles of immune escape and effector function in our observations.

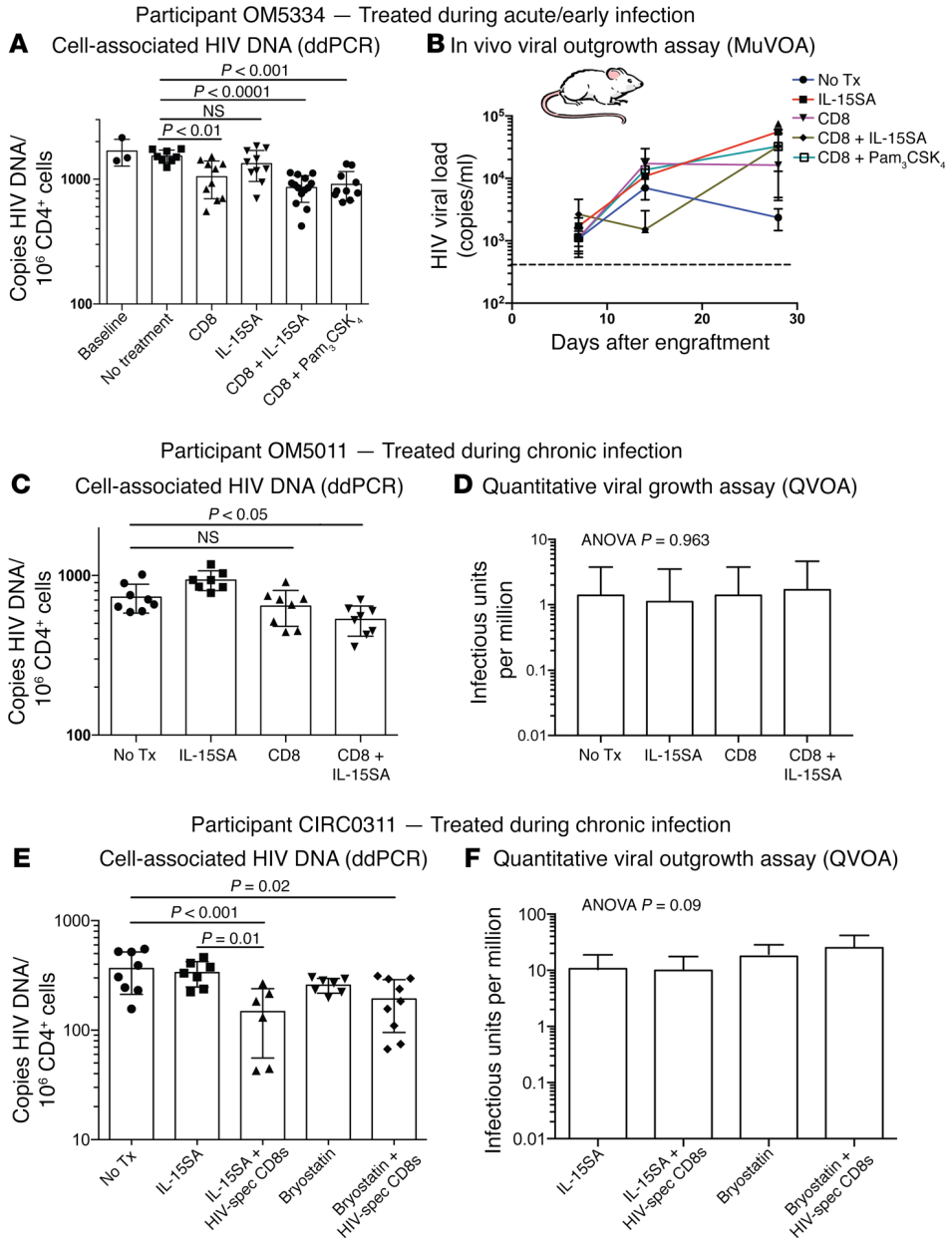

Figure 2. Ex vivo CD8⁺ T cells in combination with IL-15SA, Pam_3CSK_4, or bryostatin, drive reductions in HIV DNA but not intact-inducible HIV reservoirs. (**A**) CD8⁺ T cells from participant OM5334, treated during acute/early infection, were cultured in a HIVE assay with IL-15SA or Pam_3CSK_4, as indicated. ddPCR results show the mean ± SD, with *P* values calculated by 1-way ANOVA with Tukey's multiple comparison tests. (**B**) CD4⁺ T cells isolated from HIVE assay were injected into 3 NSG mice per condition. Shown are the mean ± SEM viral loads, indicating no significant differences in time to viral rebound. (**C**) ddPCR results for participant OM5011, treated during chronic infection. Treatment with CD8⁺ T cells + IL-15SA in this HIVE assay resulted in significant decreases in HIV DNA ($P = 0.05$). (**D**) QVOA results from the HIVE assay in **C**, showing estimated IUPM ± 95% CIs. (**E**) CD8⁺ T cells from participant CIRC0311, treated during chronic infection, were expanded following HIV peptide stimulation, then used in HIVE assays with IL-15SA or bryostatin; treatment with LRA + CD8⁺ T cells led to significant decreases in HIV DNA for both IL-15SA and bryostatin ($P < 0.05$). (**F**) QVOA from CD4⁺ T cells purified from the CIRC0311 HIVE assay shows no decrease in IUPM between LRA-only and LRA + CD8⁺ T cells conditions. NS, not significant.

Combinations of HIV-specific CD8⁺ T cell clones targeting nonescaped epitopes with an IL-15SA and/or a TLR2 agonist fail to reduce infectious reservoirs. Participant OM5011, tested in the above ex vivo CD8⁺ T cell HIVE assays, possessed a CD8⁺ T cell response to the HIV-Gag HPVHAGPIA (HA9) epitope. By single-genome sequencing we found this epitope was wild type in 10 out of 10 autologous proviral sequences. We therefore isolated an HA9-specific CD8⁺ T cell clone to use as a nonescaped CD8⁺ T cell effector. This CD8⁺ T cell clone degranulated in response to cognate peptide as measured by CD107a cell-surface expression (Figure 3A), and exhibited potent elimination of autologous CD4⁺ T cells that had been activated and superinfected with HIV JR-CSF (Figure 3B). In the HIVE assay, we observed a modest but significant reduction in cell-associated HIV DNA following a triple combination treatment with CD8⁺ T cell clone plus IL-15SA and Pam_3CSK_4 ($P < 0.05$, Figure 3C). No changes in cell-associated HIV DNA were observed following coculture with an irrelevant, autologous, CMV-pp65-specific CD8⁺ T cell clone, with or without LRAs ($P = 0.75$, Figure 3C).

The above measures of cell-associated HIV DNA were each paired with viral outgrowth assays. Results from these assays are shown here as HIV-p24 concentrations, with each dot representing a single well of the viral outgrowth assay (Figure 3D). We did not observe reductions in frequencies of intact-inducible virus following any treatment condition with the HIV-Gag-specific CD8⁺ T cell clone. As expected, reductions were also not observed with the CMV-specific negative control CD8⁺ T cell. Thus, as with bulk ex vivo CD8⁺ T cells, the combination of this Gag-specific CD8⁺ T cell clone with IL-15SA and Pam_3CSK_4 drove reductions in levels of HIV DNA, without measurably reducing the intact-inducible reservoir.

In addition to acquiring mutations in targeted epitopes, HIV can escape from CD8⁺ T cell pressure through the fixation of epitope-flanking mutations that affect epitope processing (39). Thus, although autologous viral sequences showed a lack of escape

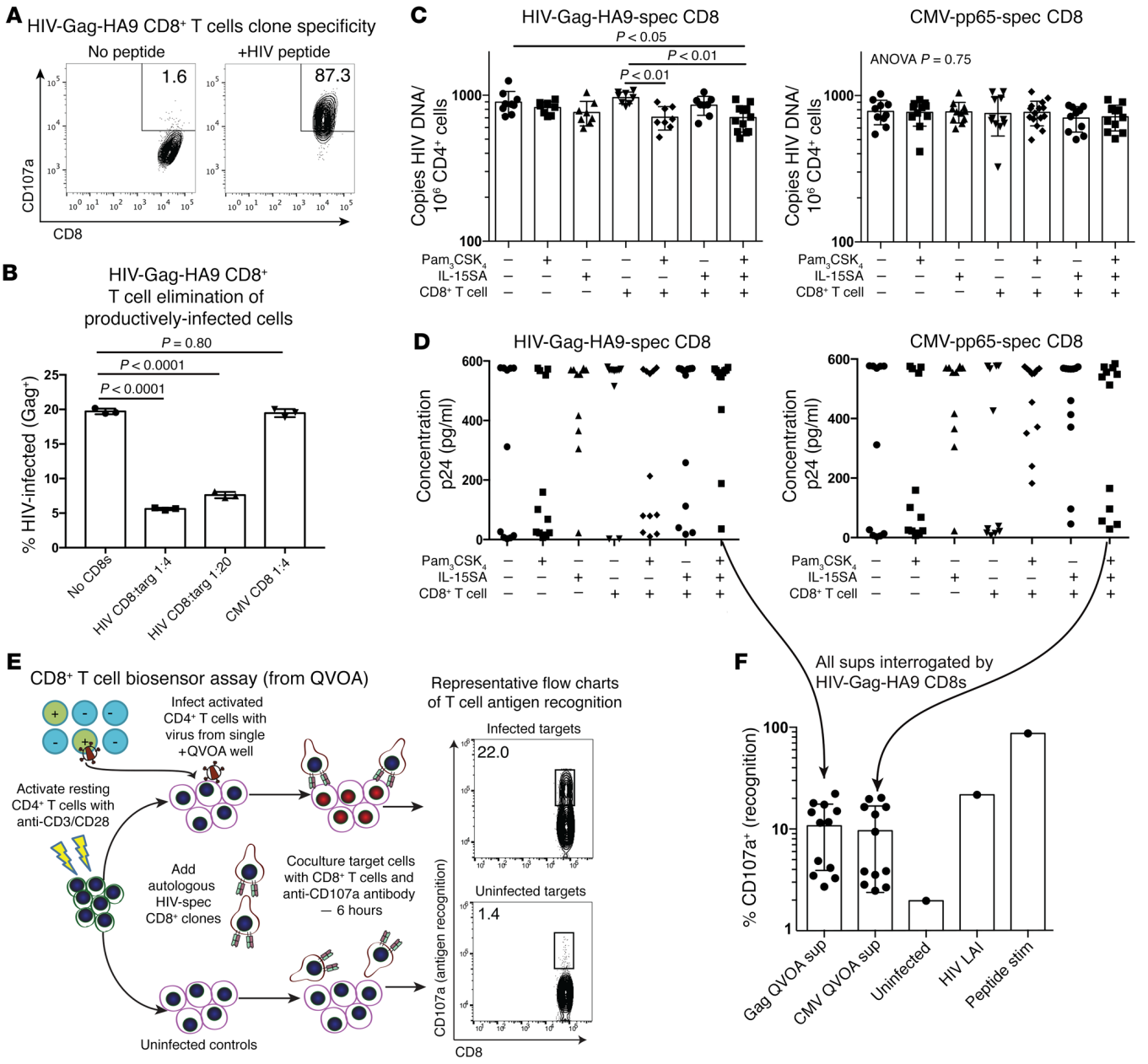

Figure 3. Combinations of a CD8+ T cell clone with IL-15SA and Pam_3CSK_4 reduces HIV DNA but fails to reduce intact-inducible HIV reservoirs. (**A**) CD8+ T cell clones degranulate in response to cognate peptide (HA9) recognition, as measured by CD107a staining. (**B**) HIV-specific CD8+ T cell clones efficiently eliminate HIV JR-CSF–infected autologous CD4+ T cells, while CMV-specific CD8+ T cell clones do not. (**C**) ddPCR results showing the mean ± SD from CD4+ T cells cocultured with autologous HIV-Gag-HA9-specific CD8+ T cell clones (left panel), or CMV-pp65-specific (right panel) CD8+ T cell clones, along with the indicated combinations of IL-15SA and Pam_3CSK_4 in HIVE assays. *P* values were calculated by 1-way ANOVA with Tukey's multiple comparison test. (**D**) p24 ELISA concentrations in QVOA wells following the HIVE assay. No statistically significant differences were observed. (**E**) Schematic of a CD8+ T cell biosensor assay to determine whether CD8+ T cell clones recognize HIV from positive wells of the QVOA. (**F**) CD8+ T cell biosensor assay demonstrates that virus from positive-outgrowth-well supernatants (sups) of the HIV-Gag-specific CD8+ T cell–treated and CMV-specific CD8+ T cell–treated conditions are equally well recognized by the HIV-Gag-specific CD8+ T cell clone HA9, ruling out CD8+ T cell escape in this assay.

mutations at the HA9 epitope targeted by this CD8+ T cell clone, the possibility remained that other mechanisms of escape may have limited its ability to reduce the infectious viral reservoir. We therefore utilized a CD8+ T cell biosensor assay to directly interrogate the ability of the Gag-HA9 CD8+ T cell clone to respond to virus isolated from p24+ wells of the QVOA — that is, viruses from infected cells that the CD8+ T cell clone had failed to eliminate during the HIVE assay (assay schematic, Figure 3E). In Figure 3F, each dot represents the percentage of CD8+ T cell clones that degranulated (CD107a+) following coculture with autologous CD4+ T cells that had been infected with virus from a single QVOA well. The peptide stimulation condition served as a positive control for the specificity of the Gag-specific CD8+ T cell, and HIV LAI served as a positive control for infected cell recognition. By comparing the ability of the Gag-specific CD8+ T cell clone to recognize QVOA supernatants from the Gag-specific CD8+ T cell HIVE assay ver-

sus the CMV-pp65-specific CD8+ T cell HIVE assay (Figure 3D) we were further able to evaluate whether virus that had survived the Gag-specific CD8+ T cell HIVE assay had been selected for putative escape mutations. We observed recognition above background (uninfected control) of virus from all 24 QVOA wells (12 each from Gag-specific-CD8+ T cell HIVE and CMV-specific CD8+ T cell HIVE). Variability in the levels of recognition were likely due to variable levels of infection, and were not different between the Gag-specific and CMV-specific CD8+ T cell QVOA supernatants (Figure 3F). These data corroborate our sequencing data showing a lack of variability in this epitope, ruling out a role for immune escape in the inability of this CD8+ T cell clone to reduce the intact-inducible reservoir.

Combinations of HIV-specific CD8+ T cell clones targeting nonescaped epitopes with bryostatin further reduce HIV DNA without reducing infectious reservoirs. We next tested whether combination of the HIV-Gag-HA9-specific CD8+ T cell clone with a more potent LRA, bryostatin (40, 41), could drive reductions in intact-inducible reservoirs. CD4+ T cells were stimulated with bryostatin, and then extensively washed to avoid bryostatin-associated impairment of CD8+ T cell function, as has been previously reported (42–44). In this HIVE assay, we observed a significant decrease in levels of cell-associated HIV DNA in the presence of CD8+ T cells ($P = 0.01$ for bryostatin vs. bryostatin + CD8+ T cells, Figure 4A). This decrease in HIV DNA was, again, not associated with a measurable reduction in intact-inducible virus as measured by QVOA (Figure 4B). We repeated this experiment using target cells from a different participant visit time point, focusing on the no treatment, bryostatin, and bryostatin plus Gag-specific CD8+ T cell conditions, and increased replicates and dilutions in the QVOA assay to improve statistical power. As before, we observed reductions in HIV DNA (copies per million CD4+ T cells: bryostatin, 240.0 ± 19.5; bryostatin + CD8+ T cells, 102.0 ± 32.0; $P < 0.0001$, data not shown), with no reduction in intact-inducible virus (Figure 4C). As predicted by the cytotoxicity of this CD8+ T cell clone (Figure 3B), and the lack of detection of escape mutants, the HA9-specific CD8+ T cell clone eliminated autologous activated CD4+ T cells that had been newly superinfected with virus from a p24+ QVOA well — that is, virus derived from cells that the CD8+ T cell clone had failed to kill during the HIVE assay (Figure 4, D and E). Thus, the inability of these CD8+ T cells to eliminate intact-inducible virus in the HIVE assay cannot be attributed to immune escape on the part of the virus, nor to functional deficiency on the part of the CD8+ T cell.

We next extended our results to an additional participant, OM5267. We generated 3 HIV-specific CD8+ T cell clones, specific for (a) the HLA-B62-restricted HIV-Nef epitope RMRRAEPAA (RA9), (b) the HLA-Cw08-restricted HIV-Nef epitope AAVDLSHFL (AL9), and (c) the HLA-B27-restricted HIV-Gag epitope IRLRPGGKK (IK9). The abilities of these CD8+ T cell clones to degranulate in response to peptide were confirmed by flow cytometric detection of CD107a the day prior to performing a HIVE assay (Figure 4F). We observed that the combination of bryostatin with each of the 3 HIV-specific T cell clones tested resulted in significant depletions in the frequencies of cells harboring HIV DNA (no treatment [No Tx] vs. bryostatin + CD8+ T cell clone, Figure 4G). For the RA9- and IK9-specific CD8+ T cells, decreases in HIV DNA were also significant relative to the bryostatin-alone condition (RA9, $P = 0.004$; IK9, $P = 0.01$), while levels of HIV DNA were not significantly different between the bryostatin-alone and bryostatin plus AL9 CD8+ T cell condition ($P = 0.33$). These differential effects on HIV DNA corresponded to epitope escape profiles (see below). Despite these reductions in HIV DNA with RA9- and IK9-specific CD8+ T cells, we did not detect corresponding reductions in intact-inducible virus (Figure 4H).

We next sequenced CD8+ T cell epitopes in virus from p24+ wells of the QVOA assay shown in Figure 4H, to assess the potential role of immune escape in the observed results. While variants were not observed for the Gag-IK9 epitope (data not shown), a number of variants were observed for the RA9 and AL9 epitopes (Figure 4I); these epitopes were sequenced from both the bryostatin plus RA9 and bryostatin plus AL9 conditions to cross-control for the selection of escape variants in the HIVE assay (which was not observed). The variant peptides were synthesized and tested against the corresponding CD8+ T cell clones in a CD107a degranulation assay. A lack of recognition was observed for each of the AL9 epitope variants, whereas recognition of the wild-type epitope remained robust; these AL9 variants were therefore defined as escape mutants. For the RA9 epitope, the R1G and R1S variants were recognized by the CD8+ T cell clone using the same peptide concentration as the wild type, while the R4Q variant induced degranulation only at higher peptide concentrations (percentage CD107a at 0.5 μg/ml peptide: wild type 27.7%, R1G 17.5%, S1G 15.5%, R4Q 0.9%). These escape profiles correspond to the degree of HIV DNA reduction (Figure 4G), where CD8+ T cells targeting the predominately unescaped RA9/IK9 epitopes drove significant depletions in HIV DNA, whereas those targeting the approximately 71% escaped AL9 epitope were associated with only a trend towards reduction, when compared with treatment with bryostatin alone. We then performed a CD8+ T cell biosensor assay with the HIV-Gag-IK9-specific CD8+ T cell (no variants observed by sequencing), and QVOA supernatants from the Gag-IK9-CD8+ T cell plus bryostatin condition. Corroborating the sequencing data, the CD8+ T cell clone exhibited robust degranulation in response to each of these viruses. Analogous to Figure 3F, each dot in Figure 4J represents the percentage degranulation (%CD107+) of the Gag-IK9-specific CD8+ T cell to autologous CD4+ T cells infected with virus from a single QVOA well. CD4+ T cells peptide infected with HIV-LAI, HIV-NL4-3, or pulsed with cognate peptide, serve as positive controls, and uninfected cells serve as negative controls. Cells infected with supernatants from each of the QVOA wells were recognized by the Gag-IK9-specific CD8+ T cell that had been used in the HIVE assay (Figure 4J), strictly ruling out a role for immune escape in the observed inability of this clone, in combination with bryostatin, to reduce the infectious reservoir as measured by QVOA.

Combinations of CD8+ T cells targeting nonescaped epitopes with PMA/I, a cocktail of LRAs, or CD3/CD28 antibodies fail to reduce infectious HIV reservoirs. In moving from IL-15SA and Pam_3CSK_4 to bryostatin in the above experiments, we went from 2 clinically viable agents with moderate LRA activity to an agent that is probably too potent for clinical use in ART-treated participants (45, 46). Additionally, we tested histone deacetylase inhibitors (HDACi's), romidepsin and vorinostat, in combination with CD8+

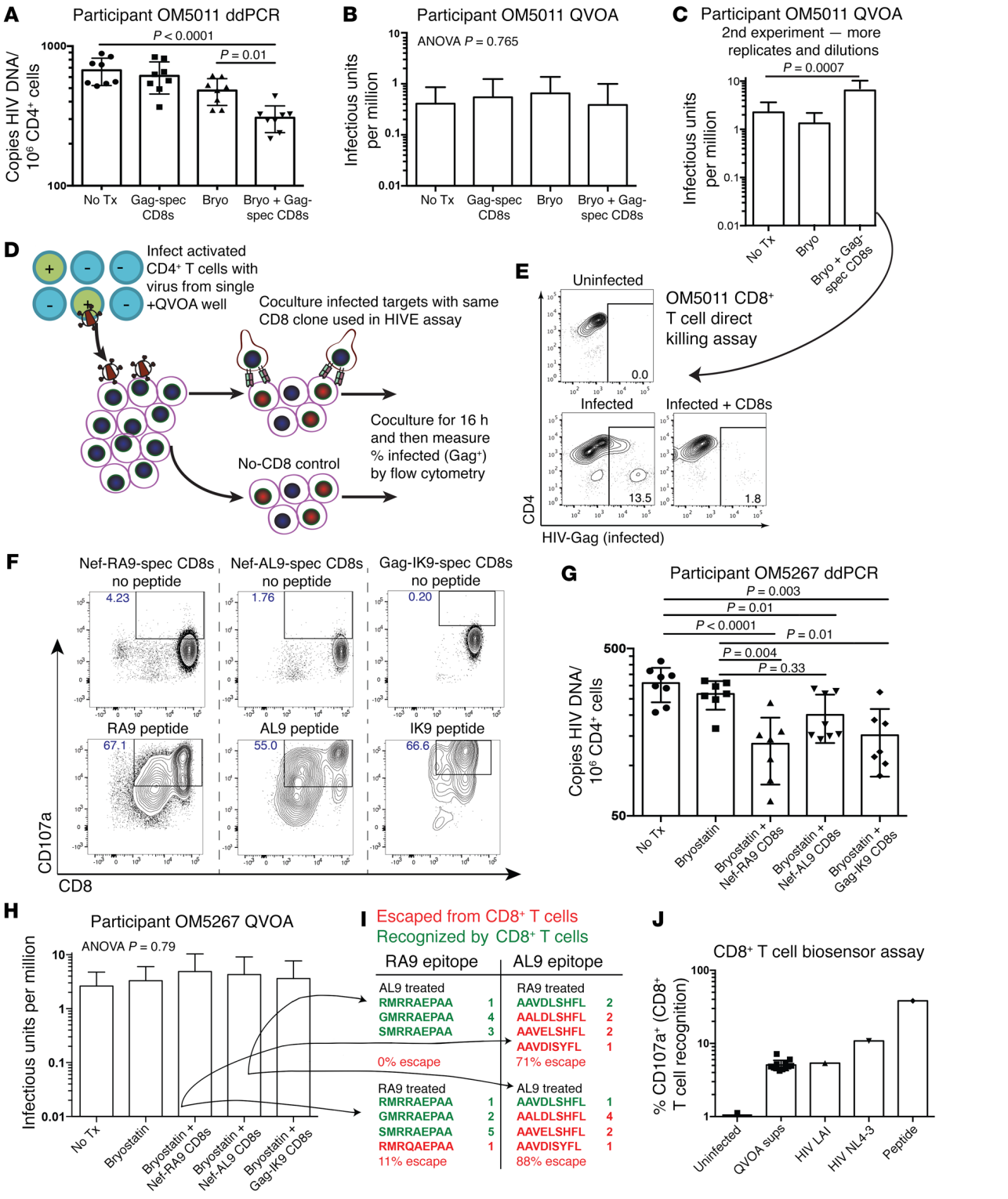

Figure 4. Combinations of HIV-specific CD8⁺ T cells with bryostatin (bryo) drive reductions in cell-associated HIV DNA without reducing the intact-inducible reservoir. (**A**) ddPCR results from a HIVE assay showing the mean ± SD. (**B**) QVOA analysis of CD4⁺ T cells, post-HIVE, show IUPM ± 95% CIs. (**C**) Higher-resolution QVOA results of a second HIVE assay using CD4⁺ T cells from the same donor but a different time point. (**D**) Schematic of CD8⁺ T cell killing assay: autologous reservoir virus from positive wells of the QVOA was used to infect activated CD4⁺ T cells from participant OM5011. Gag-specific CD8⁺ T cell clones were added to the culture to test their ability to eliminate infected cells. (**E**) Flow cytometry plot of CD8⁺ T cell killing assay indicating that the Gag-specific CD8⁺ T cell clone is able to efficiently kill CD4⁺ T cells infected with HIV from outgrowth assays. (**F**) HIV-Gag– and Nef-specific CD8⁺ T cell clones degranulate (CD107a⁺) in response to treatment with cognate peptides. (**G**) ddPCR results (mean ± SD) from a HIVE assay using bryostatin with either a Nef-RA9-specific CD8⁺ T cell, Nef-AL9-specific CD8⁺ T cell, or Gag-IK9-specific CD8⁺ T cell. (**H**) QVOA analysis of CD4⁺ T cells, post-HIVE, show IUPM ± 95% CIs. (**I**) Sequencing of viral RNA from supernatants of QVOA wells. Red = escape variants, green = nonescape variants as confirmed by degranulation assays with the CD8⁺ T cell clone. (**J**) Results from CD8⁺ T cell biosensor assay (as described above) using virus from supernatants (sups) of positive QVOA wells of the HIVE assay, treated with bryostatin + Gag-IK9-specific CD8⁺ T cells, show strong recognition of autologous reservoir virus by the Gag-IK9 CD8⁺ T cell. *P* values were calculated by 1-way ANOVA with Tukey's multiple comparison test.

Table 1. Demographics of study participants

Participant ID	Age	Gender	Ethnicity	ART Regimen	Duration of viral load <50 copies/ml (months)	Viral load (copies/ml)	Estimated time between infection and ART (months)
OM5011	47	M	W	ABC, 3TC, DTG	77	<50	Unknown
OM5334	32	M	W	ABC, 3TC, RAL	25	<50	<5 months
CIRC0311	57	M	W	3TC, ABC, ETV, DRV/r, RAL	48	<50	<11 months
OM5267	29	M	W	FTC, TDF, DRV/r, RAL	18	<50	Unknown
OM5203	39	M	W	Triumeq, DTG	42	<50	~96 months

ABC, abacavir; DRV/r, darunavir/ritonavir; DTG, dolutegravir; ETV, etravirine; FTC, emtricitabine; RAL, raltegravir; 3TC, lamivudine; TDF, tenofovir; Triumeq, abacavir/dolutegravir/lamivudine.

T cells and again did not observe reductions in intact-inducible virus (Supplemental Figure 5).

Given these results, we next set aside the consideration of clinical utility and tested whether maximal activation of CD4$^+$ T cells with PMA/I could prime cells infected with intact-inducible proviruses for CD8$^+$ T cell elimination. We observed that PMA/I alone drove a substantial reduction in levels of cell-associated HIV DNA ($P < 0.0001$, Figure 5A), with an additive effect in combination with CD8$^+$ T cells ($P = 0.02$). There was also a substantial release of viral RNA, and the addition of the CD8$^+$ T cell clone was associated with an approximately 1-log reduction in viral RNA release (Figure 5B). Despite this evidence for both latency reversal and CD8$^+$ T cell antiviral activity, we again observed no significant impact on intact-inducible virus burden as measured by QVOA (Figure 5C).

Protein kinase C (PKC) agonists, such as bryostatin, act synergistically with the bromo-domain inhibitor JQ1 and with the HDACi vorinostat, resulting in LRA activity that is almost on par with PMA/I (41). We therefore tested whether this potent LRA cocktail in combination with the nonescaped HIV Gag-HA9-specific CD8$^+$ T cell clones would result in elimination of the intact-inducible reservoir in a HIVE assay. In an attempt to further maximize CD8$^+$ T cell–mediated killing, we also blocked the coinhibitory receptors PD-1 and Tim-3 using antagonistic antibodies (47–50). We observed a trend towards an increase in HIV DNA following treatment with this cocktail alone, and a significant reduction with the addition of the CD8$^+$ T cell ($P < 0.01$) (Figure 5D); intriguingly, this increase in HIV DNA was reflected by a significant increase in IUPM ($P < 0.01$) following treatment with the cocktail alone. However, the IUPM for the CD8$^+$ T cell plus LRA plus Ab cocktail condition was not significantly different from either the No Tx or LRA plus Ab cocktail–only condition (Figure 5E). Thus, even with the use of synergistic LRA cocktails in combination with CD8$^+$ T cells targeting nonescaped epitopes, we were unable to measurably reduce the intact-inducible reservoir.

The combination of antibodies against CD3 and CD28 potently reactivates replication-competent HIV from ex vivo CD4$^+$ T cells, and can substitute for stimulation by PHA and irradiated feeder cells in QVOAs (51). We therefore assessed whether anti–CD3/CD28 stimulation in combination with both the Nef-RA9-specific CD8$^+$ T cell and Gag-HA9-specific CD8$^+$ T cell would result in elimination of the intact-inducible reservoir in a HIVE assay. We observed a significant decrease in levels of HIV DNA in the anti–CD3/CD28 plus HIV-specific CD8$^+$ T cell clones (Figure 5F, $P = 0.04$), but no accompanying reductions in IUPM (Figure 5G, overall ANOVA $P = 0.37$). For anti–CD3/CD28 and each of the other potent LRAs, potent activation of CD4$^+$ T cells was confirmed at the end of the coculture period by flow cytometry (Figure 5H). Thus, the results obtained with anti–CD3/CD28 stimulation mirrored those with PMA/I in showing significant reductions in levels of HIV DNA without a reduction in intact-inducible provirus as measured by QVOA. Thus, these data suggest that, under conditions of ex vivo latency reversal, HIV-specific CD8$^+$ T cells can eliminate a subset of defective HIV proviruses, while intact-inducible reservoirs resist CD8$^+$ T cell–mediated killing.

HIV-specific CD8$^+$ T cell elimination of defective proviruses capable of antigen expression is needed to account for decreases in HIV DNA. The HIV proviruses that are present in the CD4$^+$ T cells of an ART-treated individual can be grouped into 3 categories: (a) intact-inducible — those that give rise to viral replication following a single stimulation in a QVOA, typically comprising less than 1% of proviruses; (b) intact noninduced — intact proviruses that are not reactivated in a single stimulation in a QVOA (but which may be reactivated by subsequent stimulations), typically comprising approximately 12% of proviruses (31); and (c) defective — containing deletions or mutations that preclude the production of an infectious virus, typically comprising approximately 88% of proviruses (31). Of note, we have recently demonstrated that a subset of defective proviruses is able to express viral antigens, resulting in recognition by HIV-specific CD8$^+$ T cells (29). The magnitudes of the CD8$^+$ T cell plus LRA-mediated reductions in HIV DNA observed in the current study, along with the lack of decreases in intact-inducible proviruses as measured by QVOA, were highly suggestive of preferential elimination of cells harboring defective proviruses. However, since the proportions of defective and intact noninduced proviruses vary among different patients, the possibility remained that CD8$^+$ T cell targeting of cells harboring intact noninduced proviruses could explain decreases in HIV DNA. To distinguish between these possibilities, we utilized a previously described method (31) to determine the proportion of HIV proviruses that were intact in the reservoir of OM5011, using samples from the HIVE assay depicted in Figure 2C. We sequenced a total of 32 proviruses from these samples and observed gross deletions in each of these (Figure 6, A and B). Thus, the large majority of proviral DNA in study participant OM5011 is defective, and CD8$^+$ T cell–mediated elimination of cells harboring expressed defective proviruses is needed to account for decreases in HIV DNA in cells from this individual (Figures 2C, 3C, 4A, and 5, A and D).

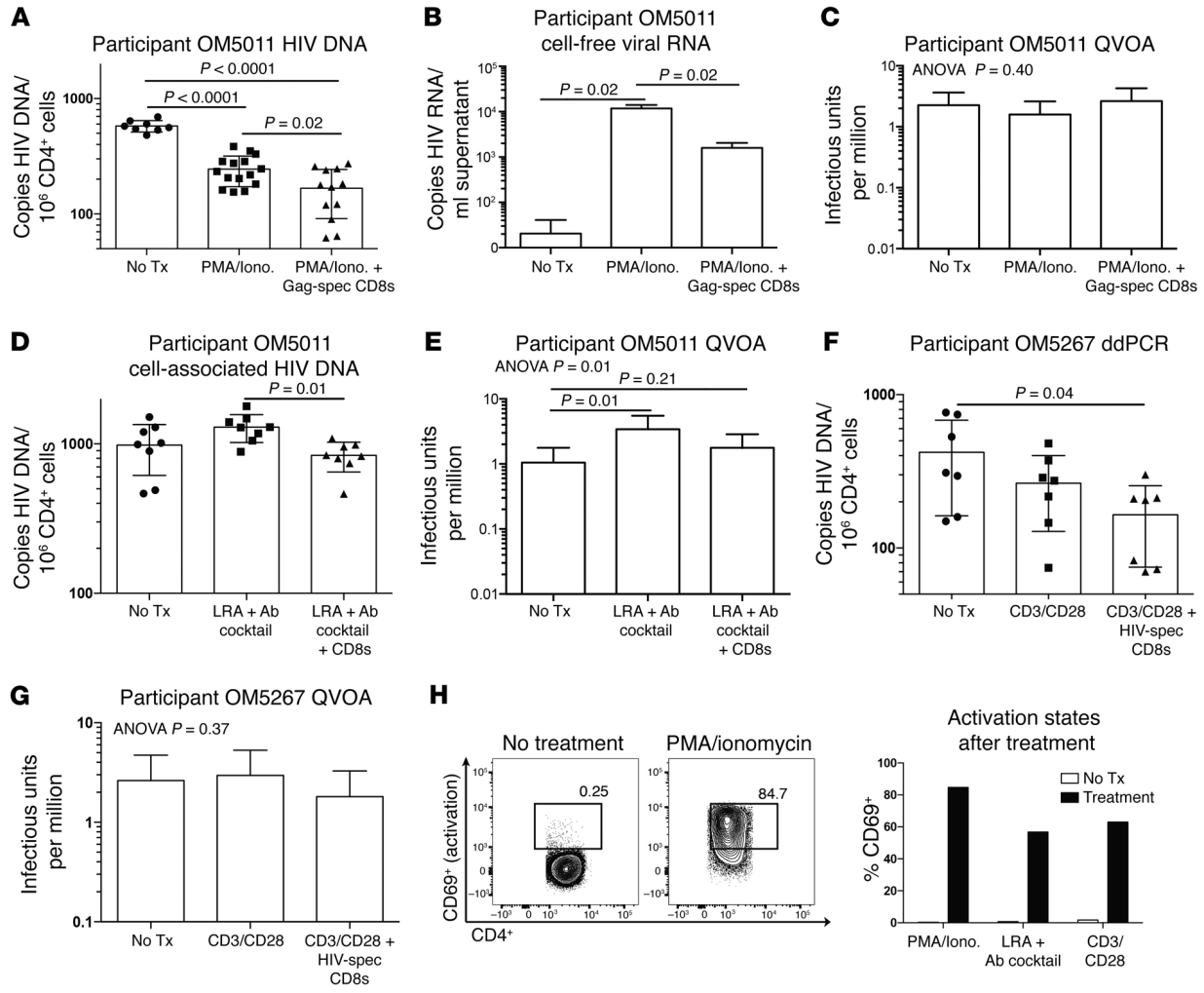

Figure 5. Combinations of HIV-specific CD8⁺ T cells with PMA/ionomycin (PMA/Iono.), an LRA + Ab cocktail, or anti–CD3/CD28 antibodies drive reductions in HIV DNA without depleting the intact-inducible reservoir. (**A**) ddPCR results from HIVE assay showing mean ± SD. Treatment with PMA/I + CD8⁺ T cells significantly depleted HIV DNA ($P < 0.0001$). (**B**) Levels of cell-free viral RNA from culture supernatant of the HIVE assay in **A**, as measured by qRT-PCR, normalized to an RNA standard. (**C**) QVOA analysis of CD4⁺ T cells, post-HIVE (corresponding to **A**), shows no significant changes in IUPM. All QVOAs show IUPM estimates ± 95% CIs. (**D** and **E**) CD4⁺ T cells from participant OM5011 were treated with a LRA + Ab cocktail of bryostatin, vorinostat, JQ1, anti-PD1, and anti-hTIM3. (**D**) ddPCR results showing mean ± SD. A trend towards an increase in HIV DNA is observed when treating with the LRA + Ab cocktail; HIV DNA is significantly depleted from these levels when CD8⁺ T cells are added to the LRA + Ab cocktail. (**E**) QVOA analysis corresponding to **D** shows no significant decreases in IUPM (LRA + Ab vs. LRA + Ab + CD8⁺ T cell, $P = 0.1$). (**F**) ddPCR results from a HIVE assay using anti–CD3/CD28 antibodies shows mean ± SD. (**G**) QVOA analysis corresponding to **F** shows no significant decreases in IUPM. (**H**) Cells treated with PMA/I, the LRA + Ab cocktail, or anti–CD3/CD28 show high levels of activation (%CD69⁺) compared with untreated cells. *P* values were calculated by 1-way ANOVA with Tukey's multiple comparison test.

Intriguingly, though none of the observed proviruses were intact, we observed that, following treatment with IL-15SA and CD8⁺ T cells the proviral population was enriched for deletions in PCR amplicon 'A' that spans the 5′ end of the viral genome (Figure 6C). OM5011 has 2 immunodominant HIV-specific CD8⁺ T cell responses that target the HPVHAGPIA (HA9, represented by CD8⁺ T cell clone used in Figures 2–5) and the ACQGVGGPGHK (AK11) Gag epitopes. Upon sequencing the PCR products from IL-15SA and CD8⁺ T cell–treated conditions, we observed that all of the deletions in these proviruses eliminated the HA9 epitope and that 12 out of 13 also eliminated the AK11 epitope (Figure 6D). This observation suggests that, in the setting of latency reversal, CD8⁺ T cells may be able to exert immunological pressure on defective proviruses, resulting in selection for proviruses with epitope deletions. These data are in line with previous reports that provide indirect evidence implicating CD8⁺ T cells in shaping the defective proviral landscape in vivo (29). Thus, we conclude that, under conditions of ex vivo latency reversal, HIV-specific CD8⁺ T cells can eliminate a subset of defective HIV proviruses, while intact-inducible reservoirs resist CD8⁺ T cell–mediated killing.

Discussion

The primary conclusion of the current study is that under controlled ex vivo conditions, combining highly functional CD8⁺ T cells targeting nonescaped epitopes with potent LRAs failed to measurably reduce intact-inducible proviruses from study par-

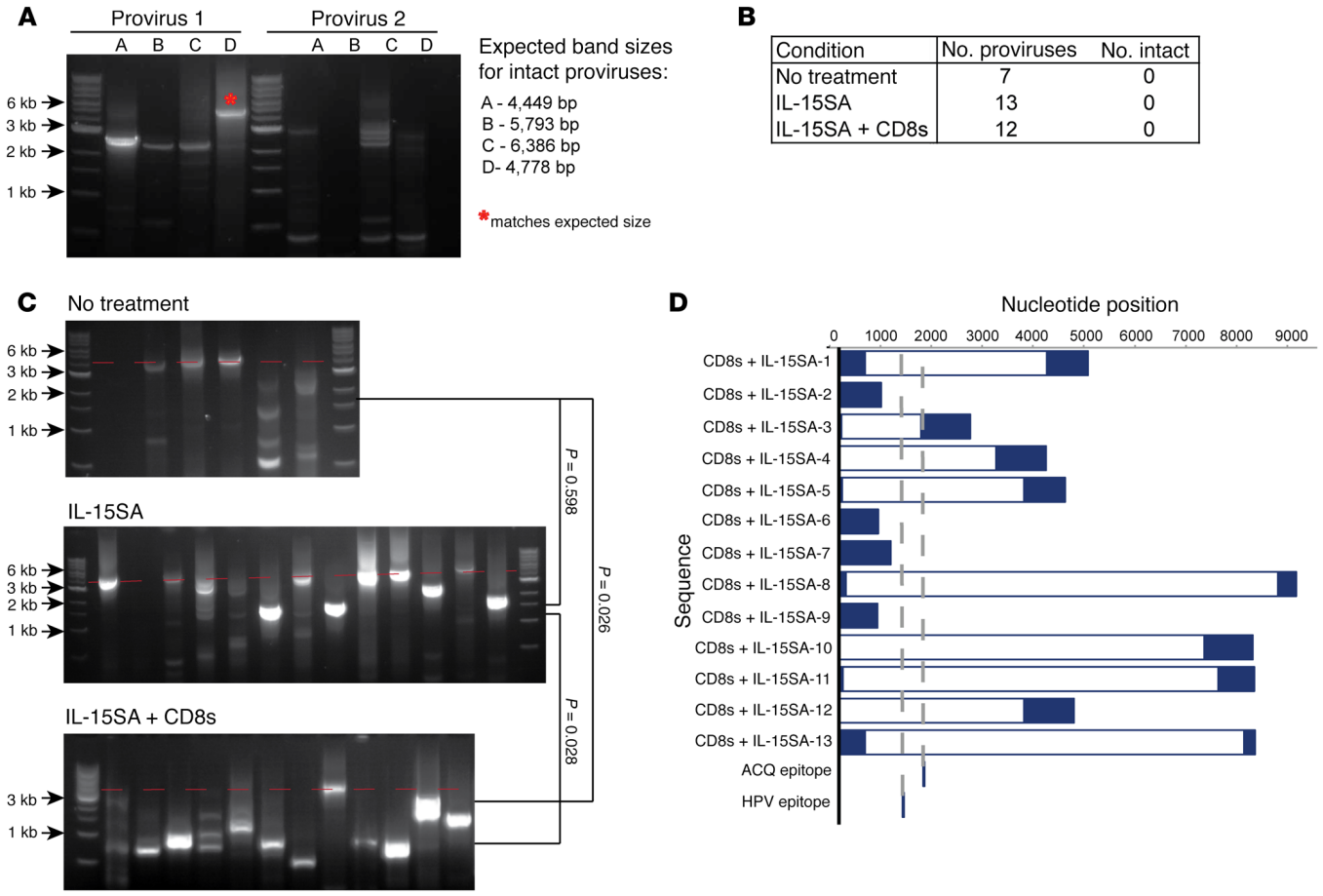

Figure 6. Characterization of HIV proviruses remaining after HIVE assay. Full-length single HIV genome amplifications (limiting dilution) were performed using the same DNA samples quantified in Figure 2C, using a previously described method (31). First-round PCRs were performed at limiting dilution and PCR reactions containing viral genomes were identified by nested PCR with *gag* primers (not shown). Each of these wells was then subjected to nested PCR over 4 overlapping regions, labeled A–D. (**A**) Shown are representative amplification products from 2 defective proviruses. Provirus 1 shows an intact region D, but a deletion affecting regions A–C. Provirus 2 does not show an intact amplicon for any of the 4 regions. (**B**) Table summarizing the results of whole-genome characterizations. Of the 32 genomes characterized, none exhibited full-length products for all 4 amplicons. (**C**) Shown are resulting amplicons from primer pair A for a number of single HIV proviruses taken from each of the treatment conditions. DNA amplicons from the IL-15SA + $CD8^+$ T cell condition were enriched for gross deletions as compared with other conditions – correct product sizes are indicated by the red line (*P* values calculated by χ^2 test). (**D**) The products shown in **C** were sequenced and are shown aligned to the HIV reference genome. The ex vivo $CD8^+$ T cells used in this HIVE assay have 2 immunodominant responses targeting HA9 and AK11 epitopes. Dashed lines indicate the positions of these epitopes in the viral genome. Proviral genomes that remain, following treatment with IL-15SA + $CD8^+$ T cells, are significantly enriched for deletions spanning $CD8^+$ T cell epitopes.

ticipant $CD4^+$ T cells. In these same experiments, we consistently observed significant reductions in levels of cell-associated HIV DNA following treatment with LRA plus $CD8^+$ T cells. The elimination of cells harboring defective HIV proviruses is needed to account for the magnitudes of these reductions, given that these outnumber intact proviruses by approximately 20 to 1 (52). This ties into our recent demonstration that antigen expression can be induced from a subset of defective HIV proviruses, allowing for recognition by $CD8^+$ T cells (29). Note, however, that a considerable proportion of defective proviruses are not capable of expressing a given antigen, imposing limits on the degrees to which $CD8^+$ T cells can reduce HIV DNA. This is exemplified by the characterization of proviruses remaining after a HIVE assay presented in Figure 6, where 12 out of 13 remaining proviruses had deletions spanning both of the targeted $CD8^+$ T cell epitopes. Thus, the observed reductions in cell-associated HIV DNA underrepresent the relative elimination of infected cells with antigen-expression-competent proviruses.

Several barriers to $CD8^+$ T cell–mediated elimination of latently infected cells are thought to contribute to the persistence of HIV reservoirs in vivo: the presence of $CD8^+$ T cell escape mutations in reservoir viruses (53, 54), a lack of antigen expression while in a latent state (1–3, 36), functional deficits in HIV-specific $CD8^+$ T cells — such as impaired cytotoxicity (55–57), and compartmentalization of infected cells in anatomical sites that are poorly accessed by $CD8^+$ T cells — such as lymph node follicles (58, 59). Our experimental design allowed us to address each of these barriers. We initially mitigated the role of immune escape by focusing our efforts on participants in whom we had identified $CD8^+$ T cell responses targeting epitopes that were predominately nonescaped in autologous proviral sequences. In several experiments we used $CD8^+$ T cell clones targeted against known epitopes, and

confirmed a lack of corresponding immune escape in virus that grew out of QVOA wells. We further directly confirmed that the CD8+ T cell clones used in these assays were able to recognize and/or eliminate autologous activated CD4+ T cells that had been newly infected with virus that had been derived from p24+ QVOA wells; i.e., virus that grew out of cells which the same CD8+ T cell clones had failed to eliminate during the HIVE assay. Thus, while immune escape will pose a challenge to the clinical translation of CD8+ T cell–based kick-and-kill strategies, it cannot explain the inability of CD8+ T cells to reduce IUPM in the current study. With respect to latency reversal, we progressed from the use of modest LRAs in initial experiments to the potent LRA bryostatin, and finally to the maximally activating agents PMA/I and anti–CD3/CD28. While a minority of intact-inducible proviruses are not reactivated following a single round of maximal reactivation (31, 60), it is unlikely that the inability of CD8+ T cells to reduce IUPM under these conditions can be attributed primarily to insufficient latency reversal. Finally, with respect to CD8+ T cell functionality, the effectors used in these experiments exhibited potent cytotoxicity against autologous CD4+ T cells that had been newly infected with either a lab isolate of HIV or autologous virus. Thus, our data lead us to propose that the inability of CD8+ T cells to eliminate cells harboring intact-inducible virus in these ex vivo assays appears to be attributable to some aspect of the functional state of the original provirus-harboring cells from the natural reservoir.

The nature of this putative resistance to CD8+ T cell–mediated elimination is currently unknown, but we propose 2 hypotheses for future investigation. The first relates to immunoevasion mediated by HIV Nef, which acts to downregulate MHC-I on infected cells, thereby diminishing recognition by CD8+ T cells (61). In productive HIV replication, Nef immunoevasion is likely limited — to some extent — by the early presentation of antigen from incoming virions prior to Nef-mediated MHC-I downregulation (within 2–6 hours of infection) (62–70). In the setting of reactivation from latency there is no parallel to this eclipse phase, and the expression of late gene products (such as Gag) will occur only after MHC-I downregulation occurs. Nef immunoevasion therefore provides a potential explanation for why the CD8+ T cells used here were unable to eliminate reactivated reservoir-harboring cells, but were able to eliminate autologous productively infected CD4+ T cells infected with virus that grew out of these same reservoirs. Nef immunoevasion may also have contributed to the apparent differential sensitivity to elimination between cells harboring intact-inducible versus defective proviruses; intact proviruses express full-length Nef, while many defective proviruses may lack functional Nef, but express sufficient antigen for CD8+ T cell recognition. A recent study by Bruner et al. reported an extensive characterization of defective HIV proviruses from patient CD4+ T cells and found a hotspot for deletions spanning *nef* (52). Among the proviruses characterized in this study, many examples exist of sequences with intact *gag* but deletions affecting *nef*. Moreover, all 43 of the hypermutated proviruses that were analyzed contained either mutated start codons or premature stop codons in *nef*. Thus, we propose that, following the reactivation of ex vivo CD4+ T cells, the majority of CD8+ T cell targets will comprise cells harboring defective proviruses, many with intact MHC-I presentation and in some cases expressing particularly antigenic defective proteins, alongside infrequent cells harboring intact proviruses that are relatively protected from CD8+ T cell recognition by Nef-mediated MHC-I downregulation. The findings of the current study may thus motivate consideration of the potential role of Nef immunoevasion in limiting the efficacy of kick-and-kill eradication strategies, as well as of a potential role of defective proviruses as immunological decoys.

Our second hypothesis is based on recent demonstrations that approximately 57% of cells harboring intact-inducible provirus are derived from expanded CD4+ T cell clones (20, 21), as well as our own evidence that CD8+ T cell pressures shape this proviral landscape in individuals on ART (29). Based on these lines of evidence, we propose that reservoir-harboring cells may have been selected for those with some intrinsic resistance to CD8+ T cell–mediated killing. A recent study reported an enrichment for proviral insertion sites into the MHC-I region in individuals on long-term ART (71), suggesting one pathway by which such resistance could be established (through disruption of antigen presentation). While further study is required to explore such possibilities, we do note a substantial representation of viruses with identical *env* V3V4 regions in p24+ wells from the post-HIVE QVOAs of the current study (~53% for OM5011 and ~90% for OM5267, Supplemental Figures 6 and 7). A recent study determined that viral isolates from ART-treated individuals that are identical in this *env* region are identical throughout the HIV genome, and thus very likely to have arisen by clonal expansion of infected cells (21). Notably, neither of the putative mechanisms of resistance proposed above was at play in the primary cell model of latency used by Shan et al. to establish the potential of the kick-and-kill approach; Nef immunoevasion was absent in this system due to the use of a Nef-deleted reporter virus, and selection for CD8+ T cell–resistant-reservoir-harboring cells that may occur over long periods of time in ART-treated individuals would not be recapitulated in this, or any other, short-term-infection in vitro latency model.

In the current study, we tested a limited number of CD8+ T cell effectors against target cells from a limited number of participants (7 and 5, respectively). Given that we took measures to overcome known obstacles to CD8+ T cell–mediated elimination, we feel that the lack of reduction in intact-inducible reservoirs that we uniformly observed comprises strong evidence for the existence of an unexpected obstacle to CD8+ T cell–mediated elimination of intact-inducible reservoirs. However, as substantial heterogeneity exists across both CD8+ T cells and reservoir composition, we do not draw the conclusion that all CD8+ T cells would show the same ineffectiveness against reservoirs from all patients under the conditions tested in our study. If, for example, Nef immunoevasion underlies our observation, then a CD8+ T cell clone that has either particularly high avidity, or is restricted by a Nef-resistant (such as HLA-C) allele, may be effective in reducing intact-inducible reservoirs. With respect to our alternative hypothesis, the reservoirs of different individuals may possess different levels of selection for CD8+ T cell–resistant cells; i.e., the reservoir in an individual with weak autologous CD8+ T cell responses would have experienced little selective pressure and may be less resistant to CD8+ T cell–mediated kick-and-kill strategies. We also acknowledge the possibility that noncytolytic effector functions of CD8+ T cells may have contributed to our observations. For example, a recent study demonstrated that the depletion of CD8+ T cells from antiretroviral-treated SIV-infected macaques resulted in elevated levels of

SIV transcripts on a per-infected-cell basis, suggesting that CD8+ T cells may act to suppress viral transcription (72). If present in vitro, such a mechanism may have counteracted latency reversal, and thus limited clearance of infected cells.

We are aware of only 2 other such studies that have assessed the impact of kick-and-kill treatments on infectious reservoirs from the ex vivo CD4+ T cells of antiretroviral-treated individuals. Both of those studies utilized clinical cell therapy products comprising mixed populations of expanded HIV-specific CD8+ T cells and activated natural killer (NK) and natural killer T (NKT) cells in combination with vorinostat, and reported reductions in viral outgrowth (14, 73). The contrast between those results and that of our current study may be attributable to a number of factors, including the use of different immune effectors and methodological differences. With respect to the latter, an important distinction is that our study used the mitogen PHA along with irradiated feeders to induce viral outgrowth in QVOA assays, whereas Sung et al. utilized irradiated feeder cells without additional stimulation. Thus, it is likely that different components of the viral reservoir were measured in these alternative approaches. We suggest that the unexpected complexity raised by the current study should prompt more widespread testing of kick-and-kill strategies against ex vivo patient CD4+ T cells, despite the challenges involved. The identification of successful cases of reservoir reductions in the HIVE assay would provide clues into the nature of potentially novel mechanisms of resistance reported in this study that, in turn, would open up novel angles from which to target the therapeutic elimination of infectious viral reservoirs in people living with HIV.

Methods

T cell cloning and maintenance. HIV-specific CD8+ T cell responses from study participants were mapped by IFN-γ ELISPOT, using 270 previously defined HIV optimal CD8+ epitopes (74). CD8+ T cell clones against the targeted peptides were established from PBMCs of HIV-infected study participants, as previously described (43). Clone specificity and activity were confirmed by degranulation assay (CD107a cell-surface expression measured by flow cytometry) within 1 day of setting up HIVE assays.

Generation of HIV-specific T cells. HIV-specific T cells were expanded and generated as previously described (75). Additional details are provided in the Supplemental Methods.

Infected cell recognition/CD8+ T cell biosensor and HIV killing assays. CD4+ T cells were enriched from PBMCs and infected with autologous reservoir HIV from p24+ QVOA wells. Parallel infections were performed with a lab isolate of HIV recognized by our CD8+ T cell clones (LAI, NL4-3, JR-CSF) (NIH AIDS Reagent Program), to serve as positive controls. Uninfected cells were maintained and used as negative controls. When infections surpassed 10%, cells were washed and cocultured with the indicated CD8+ T cell clones. For recognition assays, anti-CD107a (clone H4A3, BioLegend) antibody was added to the coculture. After a 6-hour incubation at 37°C, cells were stained with anti-CD3 (clone SK7, BD), -CD4 (clone RPA-T4, BD), and -CD8 (clone RPA-T8, BioLegend) antibodies, fixed with 2% paraformaldehyde, and analyzed by flow cytometry for CD107a cell-surface expression levels on CD8+ T cells. For killing assays, cells were stained with an amine-aqua viability dye (Thermo Fisher Scientific), anti-CD3, -CD4, and -CD8 antibodies, then fixed and permeabilized with BD Cytofix/Cytoperm, stained with Gag antibody KC57-RD1 (Beckman Coulter), and then analyzed by flow cytometry. Infected cells are defined as the percentage Gag+ within the viable CD3+CD8− population (since infected cells downregulate CD4).

HIVE assays. Detailed methods are provided in the Supplemental Methods. Briefly, resting CD4+ T cells were isolated from PBMCs by negative selection (EasySep CD4+ T Cell Enrichment Kit supplemented with HLA-DR TAC, Stemcell Technologies) following the manufacturer's instructions. Cells were analyzed by flow cytometry to ensure greater than 95% pure resting CD4+ T cells. CD8+ T cell clones were added with the LRAs indicated in the corresponding figures, and cells were cultured in XVIVO-15 serum-free medium (Lonza) supplemented with penicillin-streptomycin, L-glutamine, 0.1 nM IL-7, 1 μM tenofovir, 1 μM nevirapine, 1 μM emtricitabine, 10 μM T20, and 10 U/ml DNAse I (ProSpec) (XVIVO-10+7+ARV). CD4+ T cells were cultured with LRAs for 2 hours, then washed 3 times to prevent LRA carryover (for LRAs that have been previously associated with impairing CD8+ T cell function [e.g., bryostatin, PMA/I, HDACi's]). CD4+ T cells were then transferred to XVIVO-10+7+ARV media and cocultured with CD8+ T cell effectors. Cocultures were harvested at 4 days after initiation of coculture. CD4+ T cells from each condition were isolated twice by negative selection, then resuspended in RPMI supplemented with 10% FBS, penicillin/streptomycin, and 50 U/ml IL-2 (R10-50). Aliquots of pre- and post-CD4 enrichment were analyzed by flow cytometry to check purity, memory phenotype, and activation phenotypes and to obtain accurate cell counts. To quantify the remaining reservoir, 2×10^6 cells/condition were centrifuged and DNA (for ddPCR) was extracted from cell pellets using the Gentra Puregene kit (Qiagen), following the manufacturer's instructions, and the remaining cells were incubated overnight in R10-50 plus 4 nM IL-15SA (ALT-803), then plated out in QVOAs.

ddPCR. ddPCR was performed as previously described. See Supplemental Methods for additional details.

Viral outgrowth assays. Outgrowth assays were performed using a previously described protocol, with slight modifications (77). Details are given in Supplemental Methods.

LRAs. LRAs were used at the following concentrations: romidepsin (Sigma-Aldrich) at 40 nM; suberoylanilide hydroxamic acid at 335 nM (SAHA) (Sigma-Aldrich); bryostatin at 10 nM (Sigma-Aldrich); PMA at 50 ng/ml (Sigma-Aldrich); ionomycin at 1 μM (Sigma-Aldrich); Pam_3CSK_4 at 10 μg/ml (Invivogen); IL-15SA ALT-803 (Altor Bioscience Corporation) at 144 ng/ml; and CD3 and CD28 (OKT-3 and CD28.2 clones, Biolegend), each at 1 μg/ml.

MuVOA. Purified CD4+ T cells taken from HIVE assays were injected into NSG mice (Jackson Labs) at 10^7 cells/animal through the tail vein. Three mice were injected per HIVE assay treatment condition. HIV viral loads were measured weekly (see below). Animal experiments were performed under a protocol approved by the MGH and MIT IACUCs.

Real-time reverse transcription PCR (qRT-PCR). Viral RNA was extracted from cell-free supernatants using a Qiagen Viral RNA Mini Kit, following the manufacturer's instructions. HIV viral RNA was quantified by qRT-PCR using a probe-based method developed for the integrase single-copy assay (iSCA) (78). See Supplemental Methods for additional details.

Sequencing of Env V3V4 region. Viral RNA from p24+ wells of QVOAs was sequenced as previously described. Sequences were analyzed and assembled into phylogenetic trees using Geneious software (Biomatters).

Statistics. Statistical analyses were performed using Prism 6 (GraphPad) and methods used are reported within each figure legend.

Overall experiments were judged to be significant when the differences by ANOVA reached P less than 0.05. Additional details are given in Supplemental Methods.

Study approval. HIV-infected individuals were recruited from the Maple Leaf Medical Clinic in Toronto, Canada through a protocol approved by the University of Toronto Institutional Review Board. Secondary use of the samples from Toronto was approved through the MGH and George Washington University Institutional Review Boards. All subjects were adults, and gave written informed consent.

Author contributions

RBJ and SHH conceptualized the study. SHH, RBJ, and BDW developed the methodology. RBJ, SHH, AST, SK, YR, YCH, ARW, SM, SP, APT, CRC, DC, ABM, RT, and AB conducted the investigation. RBJ, CK, EB, BDW, HW, and EJ provided resources. RBJ and SHH wrote the original draft of the manuscript. SHH, RBJ, YCH, CMB, DFN, BDW, and RFS reviewed and edited the manuscript. RBJ, BDW, and DFN acquired funding. RBJ, BDW, CMB, CRC, and RFS supervised the study.

Acknowledgments

This work was supported by grants from the Generation Cure initiative of amfAR (109315-57-RGR); BELIEVE (NIH grant 1UM1AI26617); NIH funded Center for AIDS Research grants (P30 AI060354 and P30 AI117970), which are supported by the following NIH Co-Funding and Participating Institutes and Centers: NIAID, NCI, NICHD, NHLBI, NIDA, NIMH, NIA, FIC, and OAR; the Mark and Lisa Schwartz Foundation, and NIH R01 AI111860. The following materials were supplied by the NIH AIDS Research and Reference Reagent Program: IL-2, peptides, HIV LAI plasmid J, and MOLT-4 CCR5 cells. We are grateful to Daniel Rosenbloom for helpful discussion related to the design and interpretation of QVOA assays.

Address correspondence to: R. Brad Jones, 2300 Eye Street NW, Room 619, Washington DC, 20009, USA. Phone: 202.994.9424; Email: bradjones@gwu.edu. Or to: Bruce D. Walker, 400 Technology Square, Room 870, Cambridge, Massachusetts 02139, USA. Phone: 857.268.7073; Email: bwalker@mgh.harvard.edu.

1. Chun TW, et al. Presence of an inducible HIV-1 latent reservoir during highly active antiretroviral therapy. *Proc Natl Acad Sci U S A*. 1997;94(24):13193–13197.
2. Finzi D, et al. Identification of a reservoir for HIV-1 in patients on highly active antiretroviral therapy. *Science*. 1997;278(5341):1295–1300.
3. Wong JK, et al. Recovery of replication-competent HIV despite prolonged suppression of plasma viremia. *Science*. 1997;278(5341):1291–1295.
4. Deeks SG. HIV infection, inflammation, immunosenescence, and aging. *Annu Rev Med*. 2011;62:141–155.
5. Shan L, et al. Stimulation of HIV-1-specific cytolytic T lymphocytes facilitates elimination of latent viral reservoir after virus reactivation. *Immunity*. 2012;36(3):491–501.
6. Saleh S, et al. Expression and reactivation of HIV in a chemokine induced model of HIV latency in primary resting CD4$^+$ T cells. *Retrovirology*. 2011;8:80.
7. Spina CA, et al. An in-depth comparison of latent HIV-1 reactivation in multiple cell model systems and resting CD4$^+$ T cells from aviremic patients. *PLoS Pathog*. 2013;9(12):e1003834.
8. Novis CL, et al. Reactivation of latent HIV-1 in central memory CD4$^+$ T cells through TLR-1/2 stimulation. *Retrovirology*. 2013;10:119.
9. Sahu GK, Sango K, Selliah N, Ma Q, Skowron G, Junghans RP. Anti-HIV designer T cells progressively eradicate a latently infected cell line by sequentially inducing HIV reactivation then killing the newly gp120-positive cells. *Virology*. 2013;446(1–2):268–275.
10. Bruel T, et al. Elimination of HIV-1-infected cells by broadly neutralizing antibodies. *Nat Commun*. 2016;7:10844.
11. Lu CL, et al. Enhanced clearance of HIV-1-infected cells by broadly neutralizing antibodies against HIV-1 in vivo. *Science*. 2016;352(6288):1001–1004.
12. Halper-Stromberg A, Nussenzweig MC. Towards HIV-1 remission: potential roles for broadly neutralizing antibodies. *J Clin Invest*. 2016;126(2):415–423.
13. Lee WS, et al. Antibody-dependent cellular cytotoxicity against reactivated HIV-1-infected cells. *J Virol*. 2015;90(4):2021–2030.
14. Sung JA, et al. Expanded cytotoxic T-cell lymphocytes target the latent HIV reservoir. *J Infect Dis*. 2015;212(2):258–263.
15. Archin NM, et al. Administration of vorinostat disrupts HIV-1 latency in patients on antiretroviral therapy. *Nature*. 2012;487(7408):482–485.
16. Elliott JH, et al. Short-term administration of disulfiram for reversal of latent HIV infection: a phase 2 dose-escalation study. *Lancet HIV*. 2015;2(12):e520–e529.
17. Rasmussen TA, et al. Comparison of HDAC inhibitors in clinical development: effect on HIV production in latently infected cells and T-cell activation. *Hum Vaccin Immunother*. 2013;9(5):993–1001.
18. Maldarelli F, et al. HIV latency. Specific HIV integration sites are linked to clonal expansion and persistence of infected cells. *Science*. 2014;345(6193):179–183.
19. Wagner TA, et al. HIV latency. Proliferation of cells with HIV integrated into cancer genes contributes to persistent infection. *Science*. 2014;345(6196):570–573.
20. Bui JK, et al. Proviruses with identical sequences comprise a large fraction of the replication-competent HIV reservoir. *PLoS Pathog*. 2017;13(3):e1006283.
21. Hosmane NN, et al. Proliferation of latently infected CD4$^+$ T cells carrying replication-competent HIV-1: potential role in latent reservoir dynamics. *J Exp Med*. 2017;214(4):959–972.
22. Cohn LB, et al. HIV-1 integration landscape during latent and active infection. *Cell*. 2015;160(3):420–432.
23. Siliciano JD, et al. Long-term follow-up studies confirm the stability of the latent reservoir for HIV-1 in resting CD4$^+$ T cells. *Nat Med*. 2003;9(6):727–728.
24. Crooks AM, et al. Precise quantitation of the latent HIV-1 reservoir: implications for eradication strategies. *J Infect Dis*. 2015;212(9):1361–1365.
25. Working Group on Modelling of Antiretroviral Therapy Monitoring Strategies in Sub-Saharan Africa, et al. Sustainable HIV treatment in Africa through viral-load-informed differentiated care. *Nature*. 2015;528(7580):S68–S76.
26. Bosque A, et al. Benzotriazoles reactivate latent HIV-1 through inactivation of STAT5 SUMOylation. *Cell Rep*. 2017;18(5):1324–1334.
27. Bui JK, et al. Ex vivo activation of CD4$^+$ T-cells from donors on suppressive ART can lead to sustained production of infectious HIV-1 from a subset of infected cells. *PLoS Pathog*. 2017;13(2):e1006230.
28. Rosenbloom DI, Elliott O, Hill AL, Henrich TJ, Siliciano JM, Siliciano RF. Designing and interpreting limiting dilution assays: general principles and applications to the latent reservoir for human immunodeficiency virus-1. *Open Forum Infect Dis*. 2015;2(4):ofv123.
29. Pollack RA, et al. Defective HIV-1 proviruses are expressed and can be recognized by cytotoxic T lymphocytes, which shape the proviral landscape. *Cell Host Microbe*. 2017;21(4):494–506.e4.
30. Imamichi H, et al. Defective HIV-1 proviruses produce novel protein-coding RNA species in HIV-infected patients on combination antiretroviral therapy. *Proc Natl Acad Sci U S A*. 2016;113(31):8783–8788.
31. Ho YC, et al. Replication-competent noninduced proviruses in the latent reservoir increase barrier to HIV-1 cure. *Cell*. 2013;155(3):540–551.
32. Bosque A, Famiglietti M, Weyrich AS, Goulston C, Planelles V. Homeostatic proliferation fails to efficiently reactivate HIV-1 latently infected central memory CD4$^+$ T cells. *PLoS Pathog*. 2011;7(10):e1002288.
33. Martins LJ, et al. Modeling HIV-1 latency in primary T cells using a replication-competent virus. *AIDS Res Hum Retroviruses*. 2016;32(2):187–193.
34. Cummins NW, Sainski-Nguyen AM, Natesa-

mpillai S, Aboulnasr F, Kaufmann S, Badley AD. Maintenance of the HIV reservoir is antagonized by selective BCL2 inhibition. *J Virol*. 2017;91(11):e00012-17.
35. Wong HC, Jeng EK, Rhode PR. The IL-15-based superagonist ALT-803 promotes the antigen-independent conversion of memory CD8+ T cells into innate-like effector cells with antitumor activity. *Oncoimmunology*. 2013;2(11):e26442.
36. Jones RB, et al. A subset of latency-reversing agents expose HIV-infected resting CD4+ T-cells to recognition by cytotoxic T-lymphocytes. *PLoS Pathog*. 2016;12(4):e1005545.
37. Metcalf Pate KA, et al. A murine viral outgrowth assay to detect residual HIV type 1 in patients with undetectable viral loads. *J Infect Dis*. 2015;212(9):1387–1396.
38. Charlins P, et al. A humanized mouse-based HIV-1 viral outgrowth assay with higher sensitivity than in vitro qVOA in detecting latently infected cells from individuals on ART with undetectable viral loads. *Virology*. 2017;507:135–139.
39. Milicic A, et al. CD8+ T cell epitope-flanking mutations disrupt proteasomal processing of HIV-1 Nef. *J Immunol*. 2005;175(7):4618–4626.
40. Mehla R, et al. Bryostatin modulates latent HIV-1 infection via PKC and AMPK signaling but inhibits acute infection in a receptor independent manner. *PLoS One*. 2010;5(6):e11160.
41. Laird GM, et al. Ex vivo analysis identifies effective HIV-1 latency-reversing drug combinations. *J Clin Invest*. 2015;125(5):1901–1912.
42. Walker-Sperling VE, Pohlmeyer CW, Tarwater PM, Blankson JN. The effect of latency reversal agents on primary CD8+ T cells: implications for shock and kill strategies for human immunodeficiency virus eradication. *EBioMedicine*. 2016;8:217–229.
43. Jones RB, et al. Histone deacetylase inhibitors impair the elimination of HIV-infected cells by cytotoxic T-lymphocytes. *PLoS Pathog*. 2014;10(8):e1004287.
44. Clutton G, et al. The differential short- and long-term effects of HIV-1 latency-reversing agents on T cell function. *Sci Rep*. 2016;6:30749.
45. Hickman PF, et al. Bryostatin 1, a novel antineoplastic agent and protein kinase C activator, induces human myalgia and muscle metabolic defects: a ^{31}P magnetic resonance spectroscopic study. *Br J Cancer*. 1995;72(4):998–1003.
46. Gutiérrez C, et al. Bryostatin-1 for latent virus reactivation in HIV-infected patients on antiretroviral therapy. *AIDS*. 2016;30(9):1385–1392.
47. Jones RB, et al. Tim-3 expression defines a novel population of dysfunctional T cells with highly elevated frequencies in progressive HIV-1 infection. *J Exp Med*. 2008;205(12):2763–2779.
48. Day CL, et al. PD-1 expression on HIV-specific T cells is associated with T-cell exhaustion and disease progression. *Nature*. 2006;443(7109):350–354.
49. Trautmann L, et al. Upregulation of PD-1 expression on HIV-specific CD8+ T cells leads to reversible immune dysfunction. *Nat Med*. 2006;12(10):1198–1202.
50. Petrovas C, et al. PD-1 is a regulator of virus-specific CD8+ T cell survival in HIV infection. *J Exp Med*. 2006;203(10):2281–2292.
51. Kuzmichev YV, Veenhuis RT, Pohlmeyer CW, Garliss CC, Walker-Sperling VE, Blankson JN. A CD3/CD28 microbead-based HIV-1 viral outgrowth assay. *J Virus Erad*. 2017;3(2):85–89.
52. Bruner KM, et al. Defective proviruses rapidly accumulate during acute HIV-1 infection. *Nat Med*. 2016;22(9):1043–1049.
53. Phillips RE, et al. Human immunodeficiency virus genetic variation that can escape cytotoxic T cell recognition. *Nature*. 1991;354(6353):453–459.
54. Deng K, et al. Broad CTL response is required to clear latent HIV-1 due to dominance of escape mutations. *Nature*. 2015;517(7534):381–385.
55. Hersperger AR, et al. Increased HIV-specific CD8+ T-cell cytotoxic potential in HIV elite controllers is associated with T-bet expression. *Blood*. 2011;117(14):3799–3808.
56. Hersperger AR, et al. Perforin expression directly ex vivo by HIV-specific CD8 T-cells is a correlate of HIV elite control. *PLoS Pathog*. 2010;6(5):e1000917.
57. Migueles SA, et al. HIV-specific CD8+ T cell proliferation is coupled to perforin expression and is maintained in nonprogressors. *Nat Immunol*. 2002;3(11):1061–1068.
58. Folkvord JM, Armon C, Connick E. Lymphoid follicles are sites of heightened human immunodeficiency virus type 1 (HIV-1) replication and reduced antiretroviral effector mechanisms. *AIDS Res Hum Retroviruses*. 2005;21(5):363–370.
59. Fukazawa Y, et al. B cell follicle sanctuary permits persistent productive simian immunodeficiency virus infection in elite controllers. *Nat Med*. 2015;21(2):132–139.
60. Hosmane NN, et al. Proliferation of latently infected CD4+ T cells carrying replication-competent HIV-1: potential role in latent reservoir dynamics. *J Exp Med*. 2017;214(4):959–972.
61. Collins KL, Chen BK, Kalams SA, Walker BD, Baltimore D. HIV-1 Nef protein protects infected primary cells against killing by cytotoxic T lymphocytes. *Nature*. 1998;391(6665):397–401.
62. Yang OO, et al. Nef-mediated resistance of human immunodeficiency virus type 1 to antiviral cytotoxic T lymphocytes. *J Virol*. 2002;76(4):1626–1631.
63. Sloan RD, Kuhl BD, Donahue DA, Roland A, Bar-Magen T, Wainberg MA. Transcription of preintegrated HIV-1 cDNA modulates cell surface expression of major histocompatibility complex class I via Nef. *J Virol*. 2011;85(6):2828–2836.
64. Althaus CL, De Boer RJ. Implications of CTL-mediated killing of HIV-infected cells during the non-productive stage of infection. *PLoS ONE*. 2011;6(2):e16468.
65. Sacha JB, et al. Gag-specific CD8+ T lymphocytes recognize infected cells before AIDS-virus integration and viral protein expression. *J Immunol*. 2007;178(5):2746–2754.
66. Sacha JB, et al. Pol-specific CD8+ T cells recognize simian immunodeficiency virus-infected cells prior to Nef-mediated major histocompatibility complex class I downregulation. *J Virol*. 2007;81(21):11703–11712.
67. Sacha JB, et al. Simian immunodeficiency virus-specific CD8+ T cells recognize Vpr- and Rev-derived epitopes early after infection. *J Virol*. 2010;84(20):10907–10912.
68. Kløverpris HN, et al. Early antigen presentation of protective HIV-1 KF11Gag and KK10Gag epitopes from incoming viral particles facilitates rapid recognition of infected cells by specific CD8+ T cells. *J Virol*. 2013;87(5):2628–2638.
69. Payne RP, et al. Efficacious early antiviral activity of HIV Gag- and Pol-specific HLA-B 2705-restricted CD8+ T cells. *J Virol*. 2010;84(20):10543–10557.
70. Jimenez-Moyano E, et al. Nonhuman TRIM5 variants enhance recognition of HIV-1-infected cells by CD8+ T cells. *J Virol*. 2016;90(19):8552–8562.
71. Hadega Aamer MA, et al. HIV integration site/orientation confer selective advantage for persistence on ART [CROI abstract 304]. Conference on Retroviruses and Opportunistic infections. In Special Issue: Abstracts From the 2017 Conference on Retroviruses and Opportunistic Infections. *Top Antivir Med*. 2017;25(suppl 1):983.
72. Cartwright EK, et al. CD8(+) lymphocytes are required for maintaining viral suppression in SIV-infected macaques treated with short-term antiretroviral therapy. *Immunity*. 2016;45(3):656–668.
73. Sung JA, et al. Vorinostat renders the replication-competent latent reservoir of human immunodeficiency virus (HIV) vulnerable to clearance by CD8 T cells. *EBioMedicine*. 2017;23:52–58.
74. Goulder PJ, Walker BD. HIV and HLA class I: an evolving relationship. *Immunity*. 2012;37(3):426–440.
75. Lam S, et al. Broadly-specific cytotoxic T cells targeting multiple HIV antigens are expanded from HIV+ patients: implications for immunotherapy. *Mol Ther*. 2015;23(2):387–395.
76. Strain MC, et al. Highly precise measurement of HIV DNA by droplet digital PCR. *PLoS One*. 2013;8(4):e55943.
77. Laird GM, et al. Rapid quantification of the latent reservoir for HIV-1 using a viral outgrowth assay. *PLoS Pathog*. 2013;9(5):e1003398.
78. Cillo AR, et al. Quantification of HIV-1 latency reversal in resting CD4+ T cells from patients on suppressive antiretroviral therapy. *Proc Natl Acad Sci U S A*. 2014;111(19):7078–7083.